

Supplementary Information for

Engineering of a genetic circuit with regulatable multistability

Tingting Li,¹ Yiming Dong,¹ Xuanqi Zhang,¹ Xiangyu Ji,² Chunxiong Luo,^{1,3}
Chunbo Lou,² Haoqian M. Zhang,^{1,4,*} Qi Ouyang^{1,3,5,*}

¹Centre for Quantitative Biology and Peking-Tsinghua Joint Centre for Life Sciences,
Peking University, Beijing 100871, China

²CAS Key Laboratory of Microbial Physiological and Metabolic Engineering,
Institute of Microbiology, Chinese Academy of Sciences, Beijing 100871, China

³The State Key Laboratory for Artificial Microstructures and Mesoscopic Physics,
School of Physics, Peking University, Beijing 100871, China

⁴Center for Synthetic Biology Engineering Research, Shenzhen Institute of Advanced
Technology, Chinese Academy of Sciences, Shenzhen, 518055, China

*Correspondence: qi@pku.edu.cn (Q.O.), myelinzhang@pku.edu.cn (H.M.Z.)

Contents:

- ✧ Supplemental figures: Fig. S1~Fig. S7
- ✧ Extended modeling information
- ✧ Microfluidic chip design, fabrication and image acquisition
- ✧ Table S1. Sequences of genetic parts
- ✧ Supplementary reference

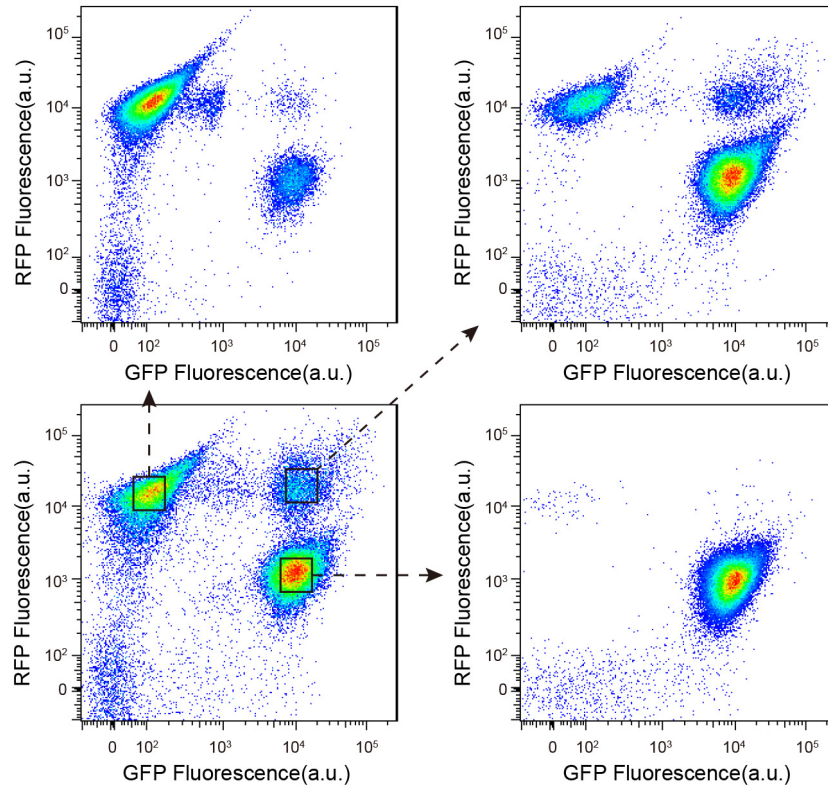


Fig. S1. FACS and re-culturing of cell populations in different states for inducible toggle switch. The sub-figure in the Lower left corner is the population distribution before sorting

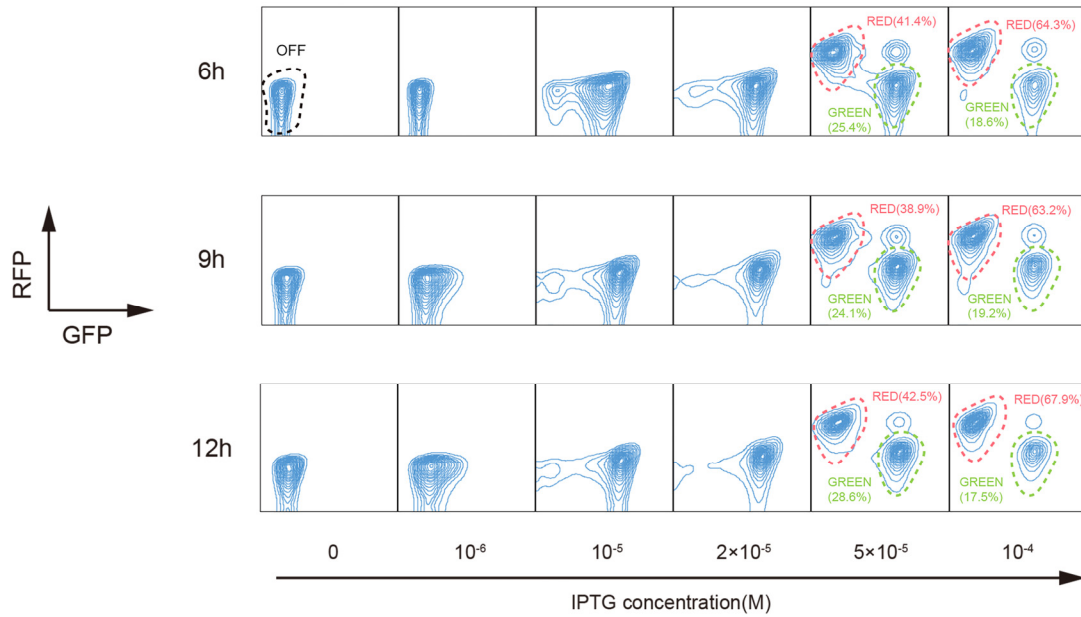


Fig. S2. Time-course measurement of the ITS after induction by an IPTG concentration gradient.

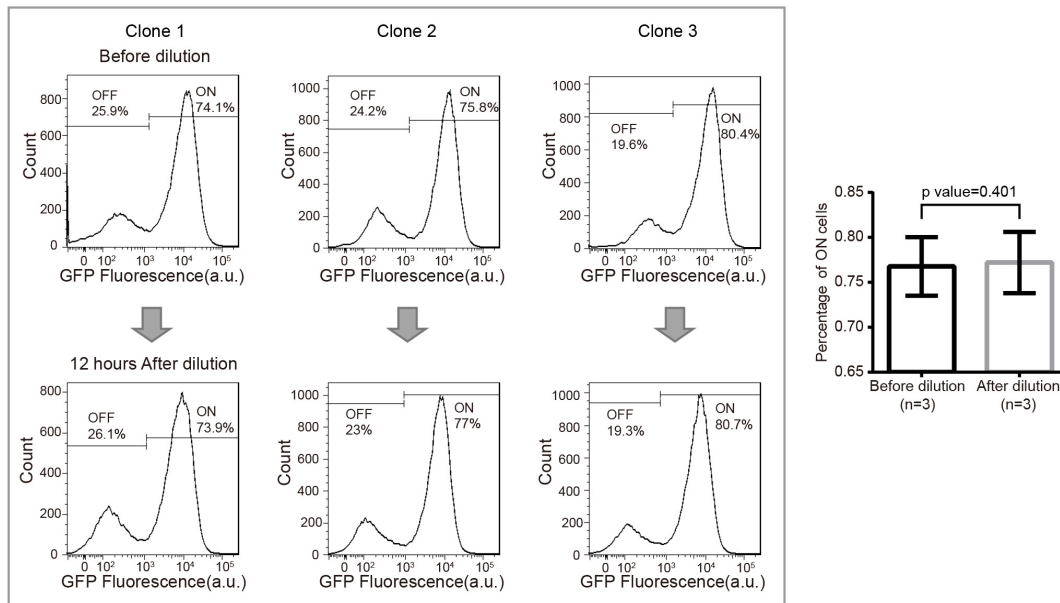


Fig. S3. Comparison of percentage of ON cells between samples before and twelve hours after dilution. Left panel: Triplicate results from the dilution experiment (Fig. 2C and Fig. 2D). Each clone was randomly selected from a separate single colony on an agar plate. All three clones showed similar ON-OFF ratios before dilution and twelve hours after dilution. Right panel: Statistical analysis for the triplicate results. The histogram with error bars indicated mean \pm SD. P value was calculated from

paired sample t test.

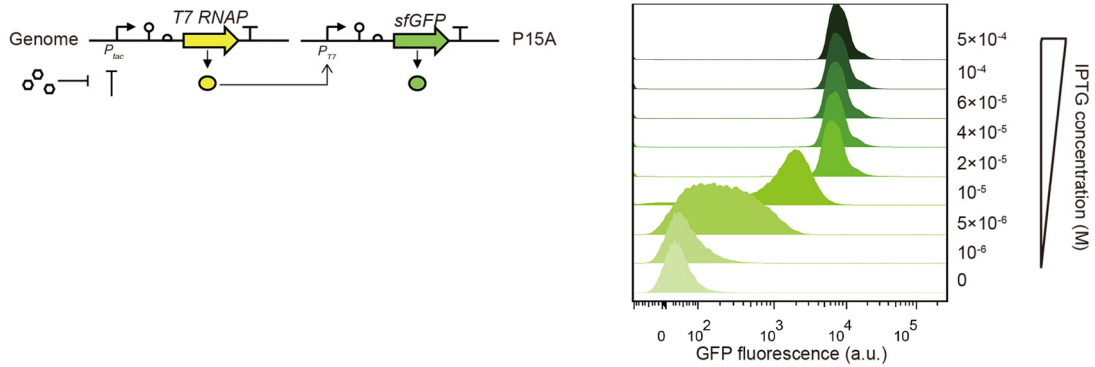


Fig. S4. Control circuit used to prove that the activation of T7 RNAP without positive feedback cannot produce bistability. Lef3t: the design of the control circuit; T7RNAP is expressed from the P_{TAC} promoter. The T7 RNAP will transcribe the downstream sfGFP from the P_{T7} promoter. Right: gradient induction of the circuit led to gradient and unimodal expression of sfGFP.

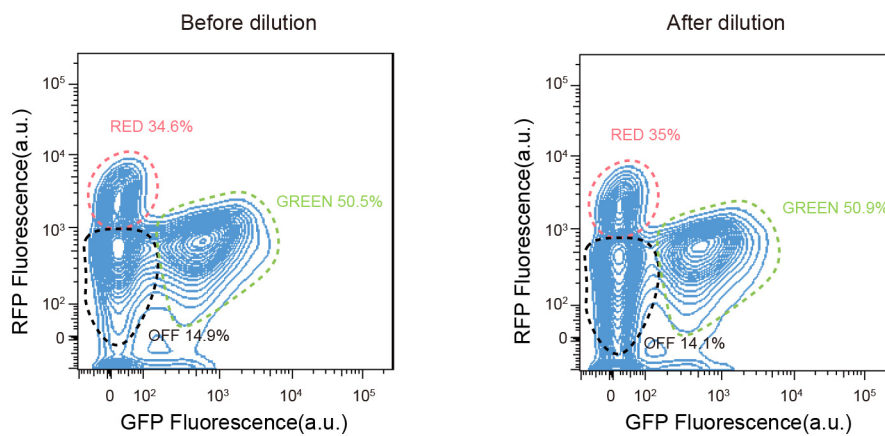


Fig. S5. Combinatorial genetic circuit exhibited a durable tristable population distribution both before dilution and after another 12 hours of culture after dilution.

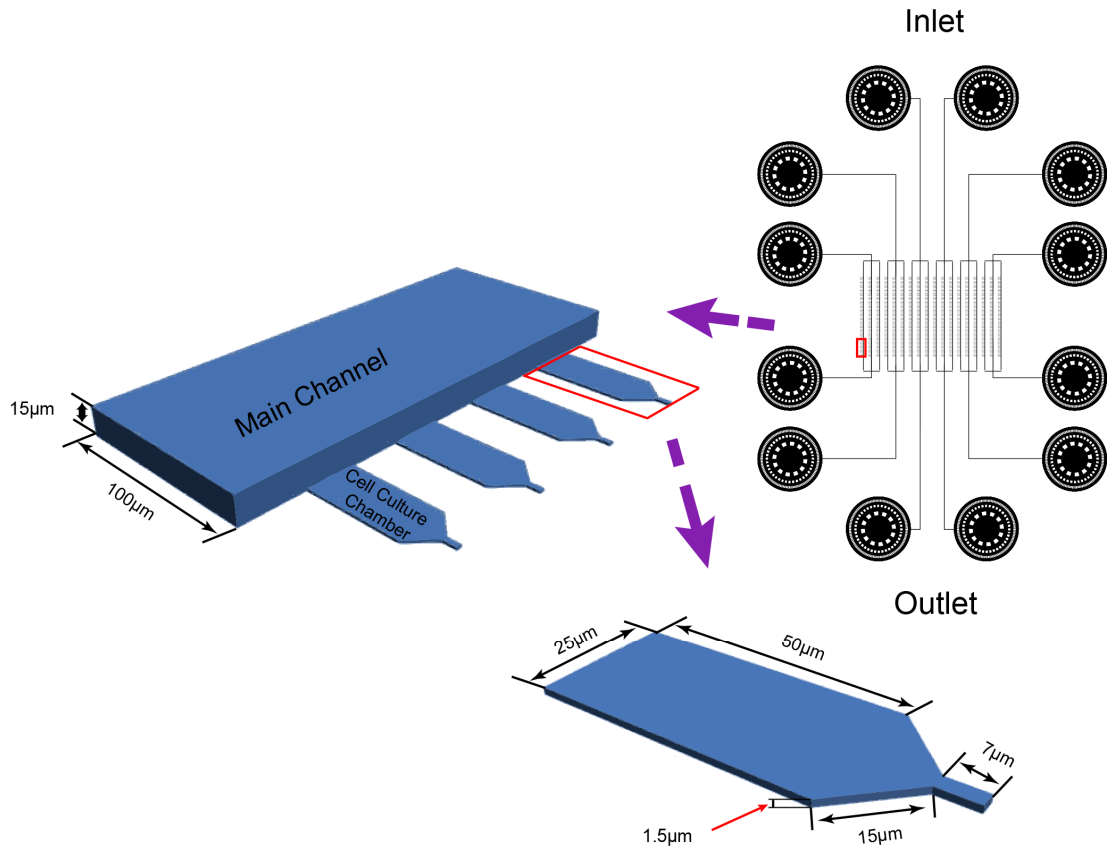
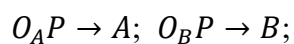
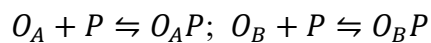
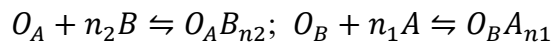


Fig. S7. Design of the microfluidics chip used to characterize the induction dynamics of ITS

Modeling

ITS model

Our circuit is designed to be a general toggle switch that consist of two proteins A and B with concentrations $[A]$ and $[B]$ respectively, which negatively regulate each other's synthesis. Additionally the synthesis of the two proteins are controlled by the concentration of $RNAP$, donated by $[P]$. Here the state of gene is represented by O , OP , O_{An} , etc. In such way, the set of chemical reactions are



$$O_A + O_AP + O_AB_{n2} = O_{A-T}; \quad O_B + O_BP + O_BA_{n1} = O_{B-T}.$$

The reactions can be described by the rate equations.

$$[O_A\dot{P}] = k_{on-AP}[O_A][P] - k_{off-AP}[O_AP];$$

$$[O_B\dot{P}] = k_{on-BP}[O_B][P] - k_{off-BP}[O_BP];$$

$$[O_B\dot{A}_{n1}] = k_{on-A}[O_B][A]^{n1} - k_{off-A}[O_BA_{n1}];$$

$$[O_A\dot{B}_{n2}] = k_{on-B}[O_A][B]^{n2} - k_{off-B}[O_AB_{n2}];$$

$$[\dot{A}] = \delta_A + g_A[O_AP] - d_A[A] - n_1[O_A\dot{A}_{n1}];$$

$$[\dot{B}] = \delta_B + g_B[O_BP] - d_B[B] - n_2[O_B\dot{B}_{n2}];$$

Where k_X denote the forward and backward rate of each reactions. g_X is the maximal production rate of protein X. , δ_A is the biochemical leakage independent on the specific reactions and d_X is its degradation rate. For simplicity, we ignore the mRNA level and take the processes of transcription and translation as a single step of synthesis. The protein binding process are much faster than the protein synthesis process that the dynamics of $[O_A\dot{P}]$, $[O_B\dot{P}]$, $[O_A\dot{A}_{n1}]$ and $[O_B\dot{B}_{n2}]$ were treated as equilibrium state. Under this assumption, one can take the time derivatives of $[O_A\dot{P}]$, $[O_B\dot{P}]$, $[O_A\dot{A}_{n1}]$ and $[O_B\dot{B}_{n2}]$ to zero, even if the system is away from steady state.

These equations can give the expression of $[O_AP]$ and $[O_BP]$.

$$[O_AP] = \frac{\frac{k_{on-AP}[P][O_{A-T}]}{k_{off-AP}}}{1 + \frac{k_{on-AP}[P]}{k_{off-AP}} + \frac{k_{on-B}[B]^{n2}}{k_{off-B}}}; \quad [O_BP] = \frac{\frac{k_{on-BP}[P][O_{B-T}]}{k_{off-BP}}}{1 + \frac{k_{on-BP}[P]}{k_{off-BP}} + \frac{k_{on-A}[A]^{n1}}{k_{off-A}}};$$

This brings the rate equations to the standard form:

$$[\dot{A}] = \delta_A + g_A[O_{A-T}] \frac{\frac{k_{on-AP}[P]}{k_{off-AP}}}{1 + \frac{k_{on-AP}[P]}{k_{off-AP}} + \frac{k_{on-B}[B]^{n2}}{k_{off-B}}} - d_A[A];$$

$$[\dot{B}] = \delta_B + g_B[O_{B-T}] \frac{\frac{k_{on-BP}[P]}{k_{off-BP}}}{1 + \frac{k_{on-BP}[P]}{k_{off-BP}} + \frac{k_{on-A}[A]^{n1}}{k_{off-A}}} - d_B[B];$$

Finally, we described the expression of the two repressors in the ITS system using the following equation:

$$\begin{aligned}\frac{dX_1}{dt} &= A_1 \cdot \frac{\frac{RNAP}{K_{RNAP}}}{1 + \frac{RNAP}{K_{RNAP}} + \left(\frac{X_2}{K_2}\right)^{n_2}} + B_1 - D_1 \cdot X_1 \\ \frac{dX_2}{dt} &= A_2 \cdot \frac{\frac{RNAP}{K_{RNAP}}}{1 + \frac{RNAP}{K_{RNAP}} + \left(\frac{X_1}{K_1}\right)^{n_1}} + B_2 - D_2 \cdot X_2\end{aligned}\quad (S1)$$

where X_1 and X_2 (nM) represent the concentrations of HKcI and cI, respectively; $RNAP$ (nM) and K_{RNAP} (nM) indicate the concentrations of T7 RNAP and its binding affinity to the promoter sequence; A_1 (nMh⁻¹) and A_2 (nMh⁻¹) account for the other elements (RBS, copy number, etc.) that control the protein expression apart from transcription; K_1 (nM) and K_2 (nM) are the binding affinities of the repressors; n_1 and n_2 are hill coefficients of repressor binding; B_1 (nMh⁻¹) and B_2 (nMh⁻¹) are the basal expression rates; and D_1 and D_2 are the decay rate constants. The first term in each line represents the regulated activity of the repressor, the second term is the basal activity and the third term is the unregulated decay of activity.

CTC model

We combined the ITS model with the SAC model to construct a combinatorial tristable circuit model.

$$\begin{aligned}\frac{dy}{dt} &= \frac{\delta + \alpha \cdot y}{1 + y} + \beta - \frac{\varphi \cdot y}{1 + \theta \cdot y} - y \\ z &= c \cdot y \\ \frac{dx_1}{dt} &= a_1 \cdot \frac{z}{1 + z + x_2^{n_2}} + b_1 - x_1 \\ \frac{dx_2}{dt} &= a_2 \cdot \frac{z}{1 + z + x_1^{n_1}} + b_2 - x_2\end{aligned}\quad (S2)$$

This combinatorial model contains three variables: y , x_1 , x_2 . In this study, we assumed that the parameter z was linearly related to y , and the value of c was 0.05 in the bifurcation analysis. For different values of β , we could solve the fixed points of y , and further solve the fixed points of x_1 and x_2 with individual fixed y .

Microfluidic chip design, fabrication and image acquisition

Microfluidic chip design: A new microfluidic chip was designed to observe the

induction dynamics of the ITS after adding IPTG (Fig. S7). There are six units in the microfluidic chip and each unit has three parallel main channels (100 μm wide, 15 μm high) so that the chip can be used to conduct experiments with six different experimental conditions or four different strain constructs simultaneously. Each unit comprises 1 inlet, 1 outlet, three main channels and 240 chambers. We also designed fences in the inlets and outlets to prevent Polydimethylsiloxane (PDMS) debris from blocking the channels. An array of cell culture chambers is connected to each side of the main channel. The height of the cell growth chambers (approximately 1.3 μm) was slightly higher than the height of an *E. coli* cell, so that the loaded *E. coli* colonies in the chambers would be recorded at the single cell level (2D). The cell culture chamber consists of three parts: a rectangular part (50 μm long, 25 μm wide) is the main growth area, a triangular part is a transition region and a small rectangular part (7 μm long, 1.5 μm wide) is akin to a “mother machine”¹.

Microfluidic device fabrication: The master mold for the device was fabricated in two layers (the first layer for the growth channels and the second layer for the main channels) by ultraviolet photolithography using standard methods. For each layer, SU-8 photoresist (Clariant Corp, Switzerland) was applied to a silicon wafer (Entegris, USA) by spin coating to appropriate thickness (corresponding to the channel height), after which patterns were created by exposing the uncured photoresist to ultraviolet light through custom quartz-chrome photomasks (Macrochem, USA). Microfluidic devices were fabricated by molding channel features into a polydimethylsiloxane (PDMS; RTV615, USA) slab and then bonding that slab to a glass coverslip. To produce the slab, dimethyl siloxane monomer (Sylgard 184, MOMENTIVE, USA) was mixed at an 8:1 ratio with curing agent (MOMENTIVE, USA), poured onto the silicon wafer master, degassed under vacuum, and cured at 65°C overnight after it was bubble-free. Holes to connect the main channels to the chambers used for medium perfusion were introduced using a hole puncher (Harris, USA), and individual chips were cut and bonded onto water-cleaned cover slips using oxygen plasma treatment on a plasma cleaner (Harrick Plasma, USA). The bonded chips were baked at 65°C overnight before use.

Microscopy and automated image acquisition: The microfluidics device was mounted onto a Nikon Eclipse Ti (Nikon, Japan) inverted microscope equipped with a 40×Plan Apo objective or 60×Plan Apo oil objective (NA 1.4, Nikon). To implement the real-time observation of the behavior of *E. coli*, we set up an auto-cultivation and observation system on the described Nikon Ti-E microscope. Images of the *E. coli* cells in the chambers were acquired under the control of NIS-Elements AR software (Nikon, Japan). The microscope scanned a series of pre-set points every 10 min, using a programmable motorized x–y stage and a PFS (perfect focus system) focus-maintaining unit. With the combination of the solution injection system and the imaging system, we were able to record the growth history of different individual bacteria at the single-cell level when these cells were exposed to LB culture medium. The temperature of the microfluidic chip was maintained at 37°C throughout the experiment using the microscope’s temperature-control system. Images were acquired every 10 min and saved as 16-bit TIFF files.

Table S1. Sequences of genetic parts

Part	Type	DNA sequence
<i>P_{T7}</i>	promoter	taatacgactcactata
<i>P_{T7M4}</i>	promoter	tataacgactcactata
<i>HKcI O</i>	operator	tgaaccataagtca
<i>cI O</i>	operator	acctctggcggtgata
<i>T7RNAP</i> RBS	RBS	ggatccccaccacagtatcgcgtaccceggg
<i>HKcI</i> RBS	RBS	ctacctaggaattagaagcaaccggaggtagcagtcgac
<i>cI</i> RBS	RBS	actaggatccagacaaggcacccatcttcaggagggtcccggg
<i>B0034</i>	RBS	agaaagaggagaaa
<i>SfGFP</i> RBS	RBS	actagagaaaggagagaataactag
(pITS)		

<i>mRFPI</i> RBS	RBS	ccgagtcagggagggtaatctgat
(pITS)		
<i>HKcl</i>	ORF	atggftcaacagaaagagcgtgaaactttctcagagcgttcgctggcctgtgataaagcgg gattacctttgcatggttaggcagcgtgatttagctgtcagcgttaaggtcacacaaaagccatt agfaaatggftcaacggggagtcataccaagaaaagacaagatggaatctctggttcgggtg ctgggaactactgctgcatactgcatggctatgctgatgatgacggfatcacggtaaatcatct atcaagatcaaatgattattatcgtgttgatgattggatgttcaggcgagcgcgggcccaggaa ccatggftccaatgaatttagaaaagataagcaattgaatatacaccgagcaggca gaatfttattaatggaaggccacaggaaagcgtaaaagtcacacggttcgctgacagcat ggagggaaacctcaatccgggagatgagatctttgtgatgtatccataacctgtttgatggcg atggcatttatgtttgtatcgggaaaacaatgcaggttaagcgcctgcaaatgcaaaagaa cagcgttcctgcatctctgacaatgccgttatgatgatgtatagagaaggtgaagaa gagcaactcaccattctagccaaagtcctcattaggcagtcfaatgattacaagcattcgga
<i>cl</i>	ORF	atgagcacaacaaaagaaaccattaacacaagagcagcgttgaggcgcacgtgccttaagc aatftatgaaaaaagaaaatgaactggcttatccaggaatctgtcgcagacaagatggg gatggggcagtcagcgttggtgctttatftaatggcatcaatgcattaaatgcttataacgccg cattgcttcacaaaattcacaagtagcgttgaagaatttagccctcaatccagagaaatc tacgagatgtatgaagcggtagtatgcagccgtcacttagaagtgagtatgattacctgtttt tctcatgttcaggcaggatgttctcactgagcttagaacctttaccaagggtgatcggagag atgggtaagcacaacaaaagccagtgattctgattctgcttgagggtgaaggtaattcc atgaccgcaccaacaggctccaagccaagcttctgacggaatgtaattctggtgacctga gcagcgtgtgagccagtgattctgcatagccagactgggggtgatgattacctcaaga aactgatcaggatagcggtcaggtgttttacaaccactaaaccacagtacccaatgatccc atgcaatgagagttgtccggttggggaaagtatcgctagtcagtgccctgaagagacgfttg gctga
<i>SfGFP</i>	ORF	atgcgtaaaggcgaagagctgtcactggtgtcgtccctattctggtggaactggatggtgatg caacggtcataagtttccgtgctggcgagggtgaaggtgacgcaactaatggtaactgac gctgaagttcatctgfactactggtaaactgccggtaccttggccgactctggtaacgacgctga cttatgggttcagtgctttgctggtatccggaccatataagcagcatgacttctcaagtcgc

		<p>catgccggaaggetatgtgcaggaacgcacgatttcctttaaggatgaeggcagctacaaaac gctgcccgaagtgaattgaaggcgataacctggtaaacgcattgagctgaaggcattga ctftaaagaagacggcaatatcctggccataagctggaatacaattttacagccacaatgttt acatcaccgccgataaacaaaaaatggcattaaagcgaatftaaaatgccacacagctgg aggatggcagcgtgcagctggctgactaccagcaaaactccaatcggtgatggtcctgt tctgtgccagacaatcactatctgagcagcaagcgttctgtctaaagatccgaacgagaaa cgcgatcatatggttctgctggagtcgtaaccgcagcggcatcacgcatggtatggatgaac gtacaaaatga</p>
<i>mRFP1</i>	ORF	<p>atggtctcctcgaagcgttatcaagagttcatgctttcaagttcgtatggaaggttccgtt agcggtcacgagttcgaatcgaagggaagggaaggctcctgacgaaggtaaccagac cgctaaactgaaagttaccaaagggtgctcctgctccttgggacatcctgcccgcagt tccagtacggttccaaagcttacgttaaacaccggctgacatcccgactacctgaaactgtcc ttcccgaagggttcaaatgggaacgtttatgaactcgaagcgggtggtgtttaccgttac ccaggactcctcctgcaagacgggtgagttcatctacaagttaaactcgtggtaccaactcc cgtccgacggtccggttatgcagaaaaaacatgggttgggaagcttccaccgaacgtatgt acccggaagacgggtctgaaagggaatcaaatgcgtctgaaactgaaagacgggtgt cactacgacgtgaagftaaaaccctacatggctaaaaaacgggtcagctgccgggtgctt acaaaaccgacatcaaacggacatcacctcccacaacgaagactacaccatcgttgaacagt acgaacgtgctgaaggctcactccaccgggtgcttaa</p>
Double terminator	T7 terminator	<p>ccagcatcaataaaacgaaaggctcagtcgaaagactgggcttctgtttatctgtgtttgt cgggtaacgctctctactagagtcacactggtcacctcgggtgggcttctcgtttatatact agagctgtaacaaagcccgaagggaagctgagttggctgctgccaccgctgagcaataacta gcataacccttgggctctaaacgggtcttgagggtttttgctgaaaggaggaactatatac cggattactagaggtcatgcttccatctgtttcttgaagat</p>
RiboJ ²	insulator	<p>agctgtcaccggatgtgctttccggtctgatgagtcctgaggacgaacagcctctacaata atthgttaa</p>

Supplemental references

- (1) Wang, P., Robert, L., Pelletier, J., Dang, W. L., Taddei, F., Wright, A., and Jun, S. (2010) Robust Growth of Escherichia coli. *Curr. Biol.* 20, 1099–1103.
- (2) Lou, C., Stanton, B., Chen, Y.-J., Munsky, B., and Voigt, C. a. (2012) Ribozyme-based insulator parts buffer synthetic circuits from genetic context. *Nat. Biotechnol.* 30, 1137–42.